MAGNETIC RESONANCE IN CHEMISTRY, VOL. 36, 407–414 (1998)

^{15}N Cross-Polarization Using the Inversion–Recovery Cross-Polarization Technique and ^{11}B Magic Angle Spinning NMR Studies of Reference Compounds Containing B—N Bonds

Christel Gervais,[1] Florence Babonneau,[1]* Jocelyne Maquet,[1] Christian Bonhomme,[1] Dominique Massiot,[2] Eric Framery[3] and Michel Vaultier[3]

[1] Chimie de la Matière Condensée, Université Pierre et Marie Curie/CNRS, 4 place Jussieu, 75252 Paris Cedex 05, France
[2] CRPHT, Centre de Recherche sur le Physique des Hautes Températures, CNRS, 45071 Orléans Cedex 2, France
[3] Synthèse et Electrosynthèse Organiques, UMR 6510, Université de Rennes 1, Campus de Beaulieu, 35042 Rennes Cedex, France

Received 30 October 1997; revised 19 January 1998; accepted 20 January 1998

ABSTRACT: Borane–ammonia complexes, trialcynylborazine and *N*-trimethylcycloborazane were characterized by ^{15}N and ^{11}B solid-state magic angle spinning (MAS) NMR. They are representative of compounds containing B—N bonds and presenting various N and B environments, either tri- or tetracoordinated. Inversion–recovery cross-polarization (IRCP), a spectral editing technique first introduced for ^{13}C, was extended to ^{15}N. For all compounds, characterized by either weak or strong ^{15}N–^{1}H dipolar couplings, the polarization inversion behavior follows the theoretical equations describing the spin dynamics associated with the IRCP sequence. This technique thus proved to be an excellent tool for identifying ^{15}N sites according to their proton environments. The isotropic chemical shift, quadrupolar coupling constant and asymmetry factor were extracted from the ^{11}B MAS NMR spectra. However, the unusual shape of the center band was tentatively related to the presence of residual ^{11}B–^{14}N dipolar coupling, which could be possibly reduced at higher fields. © 1998 John Wiley & Sons, Ltd.

KEYWORDS: solid-state NMR; ^{15}N NMR; ^{11}B NMR; cross-polarization; inversion–recovery cross-polarization; borane; borazine; borazane

INTRODUCTION

Recently, a polymer route to hexagonal boron nitride (h-BN) was developed by Fazen *et al.*[1] (Fig. 1). The borazine (**I**) ($[BH \cdot NH]_3$), is thermally polymerized to give polyborazilene (**II**).[2] This polymer can then be pyrolyzed under an inert atmosphere (argon flow) and transformed into turbostratic BN around 900 °C. The great advantage of such a polymeric synthetic approach to refractory non-oxide ceramics is the possibility of obtaining shaped materials such as fibers, films or bulk pieces.[3] It has been largely developed to produce SiC- or SiCN-based ceramics; the best example in the field is the production of the commercial Nicalon™ SiC fibers from polycarbosilane.[4]

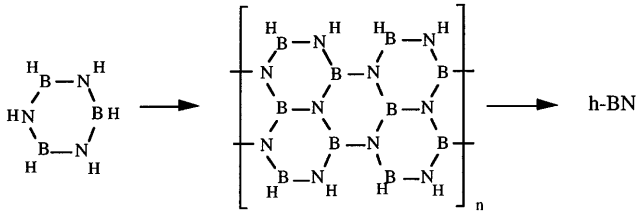

Figure 1. Schematic representation of the transformation of borazine into h-BN.

For the Si—C[5] and Si—C—N[6] systems, the influence of the polymer architecture on the structure of the final ceramics has been clearly demonstrated. It is therefore of great importance to control as much as possible the polymerization process which leads to the formation of the pre-ceramic precursor, and also the pyrolysis steps that will govern the polymer-to-ceramic conversion. Solid-state NMR studies (^{29}Si and ^{13}C) have been extremely useful for following the change in local environments during the polymerization and ceramization steps.[7]

Similar NMR studies have not yet been performed on BN pre-ceramic polymers. Fazen *et al.*[1] have studied the polymerization of borazine, using essentially mass and infrared spectrometry. Several oligomers that are formed during polymerization have been isolated, and two intermediates, diborazine, 1,2′-$(B_3N_3H_5)_2$ (**III**), and borazanaphthalene, $B_5N_5H_8$ (**IV**), have even been identified by x-ray crystallography (Fig. 2). Compound **III** can be formed by the condensation of two borazine rings and elimination of H_2, which has been clearly identified as a reaction product. The formation of **IV** strongly suggests ring opening and then re-formation of cyclic structures. This indicates that the polymerization process of borazine implies complex reactions, in which

* *Correspondence to*: F. Babonneau, Chimie de la Matière Condensée, Université Pierre et Marie Curie, 4 Place Jussieu, 75252 Paris Cedex 05, France
E-mail: fb@ccr.jussieu.fr
Contract/grant sponsor: French Ministry of Defence (DGA); *Contract/grant number*: 95-2569A.

 CCC 0749-1581/98/060407–08 $17.50

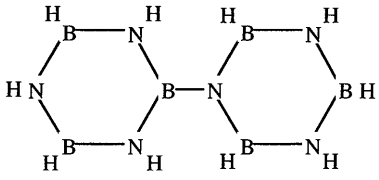

Diborazine 1.2'-$(B_3N_3H_5)_2$ (**III**)

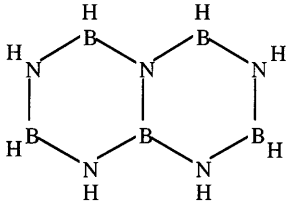

Borazanaphtalene $B_5N_5H_8$ (**IV**)

Figure 2. Schematic structures of diborazine, 1,2'-$(B_3N_3H_5)_2$ (III), and borazanaphthalene, $B_5N_5H_8$ (IV).

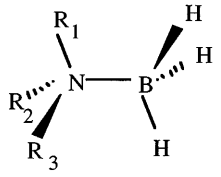

Borane-ammonia complexes : (**Va**) : $R_1 = R_2 = R_3 = H$
(**Vb**) : $R_1 = R_2 = H$, $R_3 = Me$ (**Vc**) : $R_1 = H$, $R_2 = R_3 = Me$
(**Vd**) : $R_1 = R_2 = R_3 = Me$ (**Ve**) : $R_1 = {}^tBu$, $R_2 = R_3 = H$

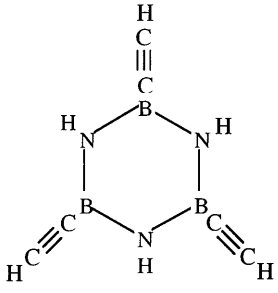

Trialcynylborazine (**VI**)

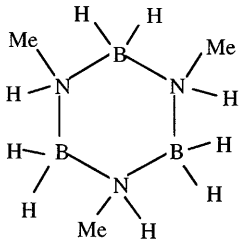

N-trimethylcycloborazane (**VII**)

Figure 3. Schematic representations of borane–ammonia complexes (V), trialcynylborazine (VI) and *N*-trimethylcycloborazane (VII).

B and N sites can experience different environments with various neighboring atoms and coordination numbers.

^{11}B and ^{15}N solid-state NMR appears to be a possible tool for characterizing the changes in environments during the polymerization process, and subsequently during the pyrolysis process. However, until now, very few NMR studies on reference compounds containing B—N bonds have been published. ^{11}B, ^{15}N and ^{1}H chemical shifts and spin–spin coupling constants [$^1J(^1H, ^{11}B)$, $^1J(^1H, ^{15}N)$, $^1J(^{15}N, ^{11}B)$] in various borane–ammonia complexes have been measured in a number of solvents.[8–10] However, little work has been done in the solid state except measurements of ^{1}H and ^{11}B T_1 for BH_3NH_3 [11], and ^{11}B chemical shifts and quadrupolar parameters for cubic and hexagonal BN.[12]

Indeed, ^{11}B and ^{15}N nuclei present their own difficulties: ^{15}N is spin-1/2, but with a very low sensitivity in natural abundance (3.8×10^{-6} compared with ^{1}H) which requires the use of cross-polarization (CP) techniques, unless enrichment of the samples can be achieved. Combined with high-power decoupling and magic angle spinning (MAS), CP is a powerful technique in solid-state high-resolution NMR that enhances weak signals from rare spins S by polarization transfer from abundant spins I (generally ^{1}H) through dipolar coupling.[13,14] Moreover, for the study of polymers, a spectral editing technique is very useful for simplifying complex spectra and to help in assigning signals. In liquid NMR, several techniques, such as DEPT and INEPT,[15] are commonly used to separate signals according to their number of directly bonded protons, taking advantage of J-couplings. However, so far in solid-state NMR, relatively few spectral editing methods have been developed, and recently a new sequence based on polarization inversion [inversion–recovery cross-polarization (IRCP) or cross-polarization combined with polarization inversion (CPPI)] has been proposed in order to obtain complete spectral editing in CP/MAS NMR.[16–21] Such a technique allows the identification of sites depending on their proton environment. Most of the work in the literature is actually related to ^{13}C studies, but recently the IRCP sequence has been successfully extended to ^{15}N and ^{29}Si studies.[22,23]

An important part of solid-state ^{11}B NMR characterizations involves borates and boron-containing glasses.[24–29] Studies on boron nitride have also been reported,[12,30] but the measurement of high-resolution spectra of half-integer quadrupolar nuclei (^{11}B, $I = 3/2$) can be difficult because of the highly anisotropic interaction of the quadrupole moment with the surrounding electric field. The resulting second-order quadrupolar broadening, which can be only partially averaged by rapid MAS, might prevent the observation of chemically non-equivalent sites. Therefore, new methods such as dynamic angle spinning (DAS),[31,32] double rotation (DOR)[33,34] and multiple quantum magic angle spinning (MQMAS)[35] were devel-

oped to remove second-order quadrupolar broadening and some workers have applied them in ^{11}B studies.[36,37]

The present study is part of a project whose main objective is the NMR characterization of the polymerization and pyrolysis processes that transform borazine into h-BN, via the formation of polyborazilene. Owing to a lack of previous studies on compounds containing B—N bonds, ^{15}N and ^{11}B solid-state NMR investigations were performed on some reference compounds with representative N and B environments that could be found in the various intermediates formed during the polymerization of borazine and pyrolysis of polyborazilene. Their schematic representations are given in Fig. 3. Borane–ammonia complexes (**V**) are examples of systems with tetracoordinated B and N atoms. They are also interesting because of their various N environments, which cover the $\equiv B \cdot R_xNH_{3-x}$ series, with $x = 0$–3. They will allow one to test the IRCP response of $^{15}NH_x$ sites ($0 \leqslant x \leqslant 3$) and to see whether this technique can help in the identification of N sites depending on their proton environments. Trialcynylborazine (**VI**) and *N*-trimethylcycloborazane (**VII**) are examples of six-membered ring structures, and are based on tricoordinated and tetracoordinated B and N sites, respectively.

The main objective of this work was to established whether it will be possible through ^{15}N and ^{11}B solid-state NMR techniques to identify various B and N sites in compounds containing B—N bonds in order to extend this study, in the near future, to the characterization of polyborazilenes.

EXPERIMENTAL

The borane–ammonia complexes, $NH_3 \cdot BH_3$ [38] (**Va**) and $MeNH_2 \cdot BH_3$ [39] (**Vb**), the trialcynylborazine[40] (**VI**) and the *N*-trimethylcycloborazane[41] (**VII**) were prepared following procedures proposed in the literature. The borane–ammonia complexes $Me_2NH \cdot BH_3$ (**Vc**) $^tBuNH_2 \cdot BH_3$ (**Ve**) and $Me_3N \cdot BH_3$ (**Vd**) were purchased from Aldrich.

Solid-state ^{15}N CP/MAS experiments were performed at room temperature on a Bruker MSL-300 spectrometer at a frequency of 30.41 MHz (^{15}N) and 300.13 MHz (^1H), using a Bruker CP/MAS probe. Proton decoupling was always applied during acquisition. Solid samples were spun at 5 kHz, using 7 mm ZrO_2 rotors filled in a glove-box under a dried argon atmosphere. All ^{15}N CP/MAS experiments were performed under the same Hartmann–Hahn match conditions, set up by using a powdered sample of NH_4NO_3: both r.f. channel levels $\omega_{1H}/2\pi$ and $\omega_{15N}/2\pi$ were carefully set so that $|\omega_{1H}|/2\pi = |\omega_{15N}|/2\pi = 42$ kHz. The spectra were accumulated in order to achieve a reasonable signal-to-noise ratio, with 360–1600 FIDs. A spectral width of 25 kHz was used with 4K data points for the FID. The repetition time was 10 s. Chemical shifts were referenced to solid NH_4NO_3 [10% ^{15}N enriched sample, δ_{iso} ($^{15}NO_3$) = −4.6 ppm compared with CH_3NO_2 ($\delta = 0$ ppm)]. For each sample, ^{15}N CP/MAS spectra were recorded with different contact times t_c, ranging from 100 μs to 40 ms. For the IRCP experiments, the contact time was chosen in order to maximize the polarization of the ^{15}N nuclei and the spectra were recorded with various inversion times t_i from 5 μs to 7 ms.

Solid-state ^{11}B MAS experiments were performed at room temperature on a Bruker MSL-400 spectrometer at a frequency of 128.28 MHz, using a Doty CP/MAS probe, with no probe background. Spectra were recorded with and without proton decoupling. Solid samples were spun at 8–10 kHz, depending on the sample, using 5 mm ZrO_2 rotors filled in a glove-box under a dried argon atmosphere. All ^{11}B chemical shifts were determined relative to liquid BF_3OEt_2 ($\delta = 0$ ppm) and the number of FIDs varied from 64 to 112. A 1 μs single-pulse excitation was used [$t_{90°}$ (BF_3OEt_2) = 8 μs], with repetition times from 2 to 5 s. Spectral widths of 125 kHz were used with 4K data points for the FIDs.

The FIDs were then analyzed with the Bruker WIN-NMR program and simulations of spectra were done using the WIN-FIT program.[42]

RESULTS AND DISCUSSION

^{15}N CP and IRCP MAS NMR studies

Figure 4 shows CP/MAS spectra of **Vd** and **VI** as examples. The isotropic chemical shifts obtained for all the studied compounds are summarized in Table 1. It shows a large chemical shift range: between −325 and −364 ppm for the tetracoordinated N atoms and at −267 ppm for the tricoordinated N atoms. These values are in good agreement with those found in solution,[10,43] and show that tri- and tetracoordinated N atoms can be easily distinguished based on isotropic chemical shift considerations. Within the $Me_xNH_{3-x} \cdot BH_3$ ($0 \leqslant x \leqslant 3$) series, characterized by only tetracoordinated N sites, a slight upfield shift is observed when x increases; however, clear identification of NH_x sites based on chemical shift considerations seems difficult, especially in the polyborazilene spectra, for which broader and possibly overlapping lines are expected. This led us to investigate the ^{15}N IRCP response of the various compounds to see whether site

Table 1. ^{15}N chemical shifts extracted from the ^{15}N CP MAS NMR spectra

Compound	δ_{iso} (^{15}N) (ppm)
$NH_3 \cdot BH_3$ (**Va**)	−364
$MeNH_2 \cdot BH_3$ (**Vb**)	−361
$Me_2NH \cdot BH_3$ (**Vc**)	−358
$Me_3N \cdot BH_3$ (**Vd**)	−347
$^tBuNH_2 \cdot BH_3$ (**Ve**)	−325
$B_3N_3C_6H_6$ (**VI**)	−267
$(MeNH \cdot BH_2)_3$ (**VII**)	−359

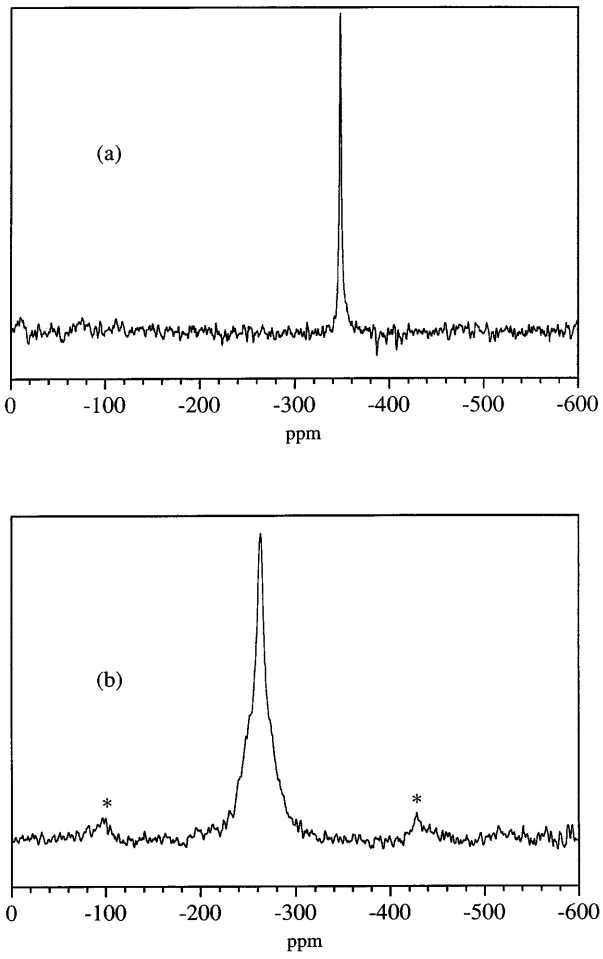

Figure 4. Experimental ^{15}N CP/MAS spectra of (a) $Me_3N \cdot BH_3$ **(Vd)** ($t_c = 20$ ms, 600 scans and $\nu_{rot} = 5$ kHz) and (b) trialcynylborazine **(VI)** ($t_c = 10$ ms, 1000 scans and $\nu_{rot} = 5$ kHz). Asterisks indicate spinning side bands.

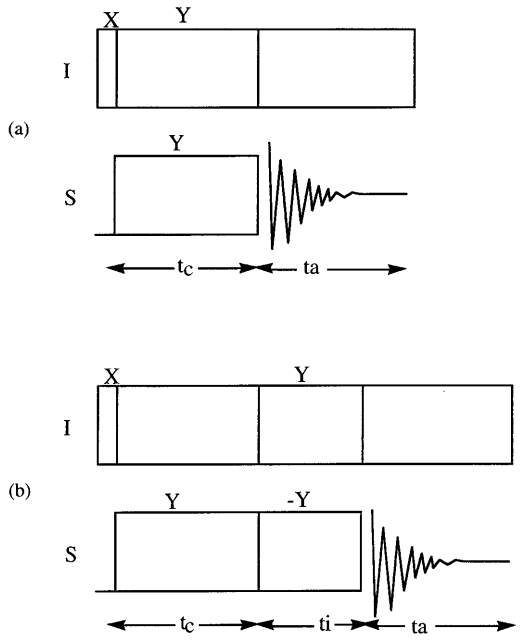

Figure 5. (a) CP sequence; (b) IRCP sequence.

identification can be achieved, based on this spectral editing technique.

In an IRCP experiment, the only modification compared with the standard CP sequence is the introduction of a phase inversion during the contact time (Fig. 5). The dynamics of inversion are similar to polarization dynamics in the standard CP sequence[44] and thus depend strongly on the *I–S* dipolar coupling. As the abundant spins *I* are typically protons, this sequence is very sensitive to the local proton environment and molecular motion. Its main advantage over the standard CP sequence is that the magnetization starts from an optimum value, then decreases and becomes negative with increasing inversion time; it is therefore easy to visualize differences in dynamics from various sites.

The different IRCP spectra of **Vc** as a function of inversion time are presented in Fig. 6. They were simulated: the chemical shift, linewidth and shape were kept constant, and only the amplitudes were fitted. Then the integrated intensities were normalized and plotted against inversion time, assuming that the magnetization reached after the contact time is nearly the maximum theoretical magnetization. The resulting polarization inversion curve is presented in Fig. 7 together with those obtained for the $Me_xNH_{3-x} \cdot BH_3$ ($0 \leqslant x \leqslant 3$) series.

Two models exist to describe the spin dynamics associated with the IRCP sequence. The first model, associated with systems with a small dipolar coupling such as non-protonated groups or systems with an important molecular motion, describes the magnet-

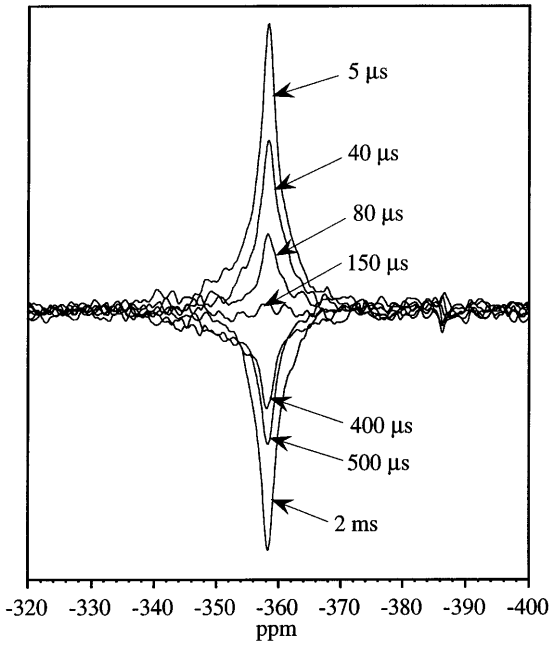

Figure 6. Evolution *vs.* inversion time of the IRCP/MAS spectra of $Me_2NH \cdot BH_3$ **(Vc)** ($t_c = 3$ ms, 360 scans, $\nu_{rot} = 5$ kHz).

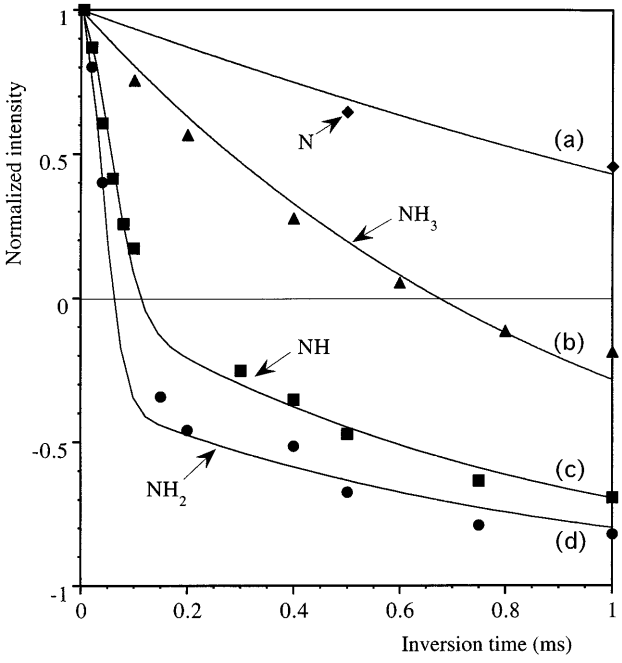

Figure 7. Evolution *vs.* inversion time of the ^{15}N IRCP/MAS NMR signal intensities for the $Me_xNH_{3-x}\cdot BH_3$ ($0 \le x \le 3$) series: (a) **Vd**; (b) **Va**; (c) **Vc**; and (d) **Vb**. Curves were fitted according to Eqn (1) for (a) and (b) and Eqn (2) for (c) and (d).

ization by a single exponential decrease:[18]

$$M_S(t_i) = M^0(t_c)\left[2\exp\left(-\frac{t_i}{T_{IS}}\right) - 1\right] \quad (1)$$

assuming $T_{IS} \ll T_{I\rho}^H$, where T_{IS} is the standard cross-polarization time which is related to the strength of the *I–S* dipolar coupling and $T_{I\rho}^H$ is the relaxation time of the protons in the rotating frame. $M^0(t_c)$ represents the polarized magnetization reached after the contact time t_c.

The second model concerns systems with a strong heteronuclear dipolar coupling such as rigid NH or NH_2 groups. In this case, the inversion of magnetization could be well described by the following equation:[17,18]

$$M_S(t_i) = M^0(t_c)\left[\frac{2}{n+1}\exp\left(-\frac{t_i}{T_D}\right) + \frac{2n}{n+1} \times \exp\left(-\frac{3t_i}{2T_D}\right)\exp\left(-\frac{t_i^2}{T_C^2}\right) - 1\right] \quad (2)$$

T_C is related to dipolar coupling to nearby protons leading to a coherent transfer of polarization;[20] T_D describes the decay caused by isotropic spin diffusion ($T_C \ll T_D$) and n corresponds to the number of directly bonded protons. The polarization inversion proceeds in two stages with different time-scales. It decreases rapidly during the first few hundred microseconds owing to transfer of magnetization with nearby protons, and then approaches the equilibrium value at a much slower rate due to spin diffusion. Equation (2) predicts a turning point for the normalized intensity at $[2/(n+1)] - 1$, corresponding to $\exp(-3t_i^2/T_C^2) \approx 0$ ($t_i \gg T_C$) and $\exp(-t_i/T_D) \approx 1$ ($t_i \ll T_D$).

Simulations of the polarization inversion curves *vs.* inversion times for various N environments are presented in Fig. 7. Curves (a) and (b) were fitted using Eqn (1) and curves (c) and (d) using Eqn (2).

^{15}NH sites. The fitted parameters T_C and T_D obtained from the simulations of IRCP curves (Fig. 8) for $Me_2NH\cdot BH_3$ (**Vc**), $B_3N_3C_6H_6$ (**VI**) and $(MeNH\cdot BH_2)_3$ (**VII**) with Eqn (2) are summarized in Table 2. The agreement factors are fairly good, > 0.98. For NH groups, Eqn (2) predicts a turning point for the normalized intensity at zero, which is clearly observed experimentally. The cross-polarization times T_C are much larger, between 50 and 80 μs, than those observed

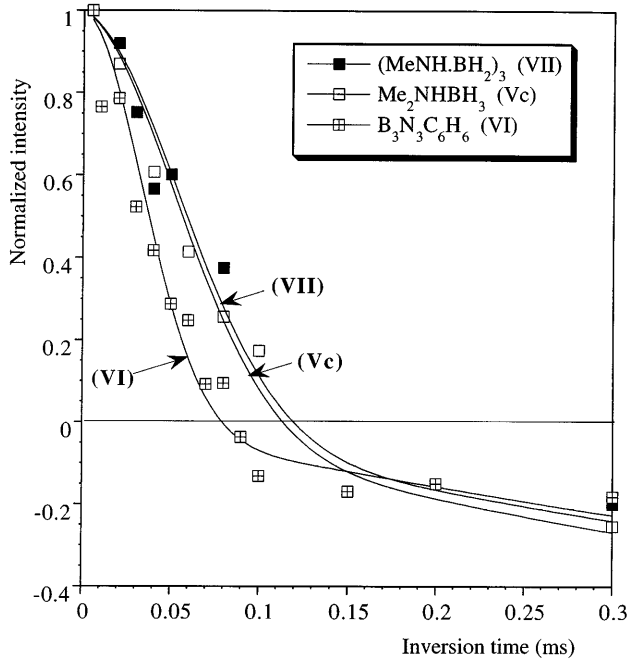

Figure 8. Evolution *vs.* inversion time of the ^{15}N IRCP/MAS NMR signal intensities of compounds containing NH groups, **Vc**, **VI** and **VII**. Curves were fitted according to Eqn (2).

Table 2. CP characteristic times extracted from the ^{15}N IRCP/MAS NMR spectra

Compound	T_c (μs)[a]	T_D (ms)[b]	T_{NH} (ms)[c]
$NH_3\cdot BH_3$ (**Va**)	—	—	1.1
$MeNH_2\cdot BH_3$ (**Vb**)	44	1.4	—
$Me_2NH\cdot BH_3$ (**Vc**)	82	0.9	—
$Me_3N\cdot BH_3$ (**Vd**)	—	—	6.1
$^tBuNH_2\cdot BH_3$ (**Ve**)	58	0.8	—
$B_3N_3C_6H_6$ (**VI**)	48	1.3	—
$(MeNH\cdot BH_2)_3$ (**VII**)	83	0.6	—

[a] Cross-polarization time from Eqn (2).
[b] Spin diffusion time from Eqn (2).
[c] Standard cross-polarization time from Eqn (1).

for rigid ^{13}CH pairs (*ca.* 10–20 μs).[17,18] This could be due to smaller dipolar coupling ($\gamma_N < \gamma_C$), but also to molecular motions of the NH group, that partially average the dipolar coupling. Indeed, the T_C values for the two tetracoordinated ^{15}N sites in **Vc** and **VII** (80 μs) are longer than that observed for the tricoordinated ^{15}N site in **VI** (50 μs). Besides possible differences in NH bonding in the various compounds, reorientation motions involving the N group can induce variations in ^{1}H–^{15}N dipolar coupling. Reorientation around the B—N bonds in borane–ammonia complexes has already been reported,[11] and can occur in **Vc**. Fluctuations of the borazane ring in **VII** could also account for a reduced value of the dipolar coupling, compared with the more rigid borazine ring in **VI**.

$^{15}NH_2$ sites. The simulation of IRCP curves for $MeNH_2 \cdot BH_3$ (**Vb**) and $^tBuNH_2 \cdot BH_3$ (**Ve**) with Eqn (2) also gives satisfactory results with a turning point for the normalized intensity at $-1/3$, as predicted by theory. The fitted T_C values are smaller then those related to NH sites in related borane–ammonia complexes, 45 μs for **Vb** and 60 μs for **Ve**; a similar behavior was reported considering CH and CH_2 sites.[17]

$^{15}N(CH_3)_3$ site. A single-exponential behavior is observed for $Me_3N \cdot BH_3$ (**Vd**), characterized with a long T_c of 6 ms.

$^{15}NH_3$ site. The magnetization behavior for $NH_3 \cdot BH_3$ (**Va**) is also well described by a single-exponential regime [Eqn (1)]. This behavior, typical of non-protonated groups, can be related to the free rotation of NH_3 groups around the B—N bond,[11] which leads to partial averaging of the ^{1}H–^{15}N dipolar coupling. This phenomenon has already been observed for $^{13}CH_3$ groups.[45] However, one can observe that T_C (1 ms) is much shorter than the value reported for $Me_3N \cdot BH_3$, indicative of a stronger ^{15}N–^{1}H dipolar coupling.

The comparison of the polarization transfer dynamics using the IRCP sequence clearly shows that it is possible to distinguish the various $^{15}NH_x$ sites according to their degree of protonation, through the various time constants related to the polarization inversion dynamics. Moreover, the different turning points observed between the two regimes of polarization inversion for NH and NH_2 entities allow a clear differentiation between these two groups. Nevertheless, possible molecular motions have to be carefully considered when analyzing the data, since they could lead to partial averaging of the ^{1}H–^{15}N dipolar coupling: the models presented to describe the evolution of magnetization during an IRCP experiment are related to rigid groups. Another difficulty arises from the choice of the contact time t_c, especially for systems with a small dipolar coupling. If t_c is too long, the signal vanishes because of proton relaxation. If t_c is too short, the magnetization reached is far from the theoretical maximum and Eqns (1) and (2) can no longer be used.

^{11}B MAS NMR studies

Chemical shielding differences between trigonal and tetragonal boron atoms are expected and have already been reported for c-BN ($\delta_{ISO} = 1.6$ ppm) and h-BN ($\delta_{ISO} = 30.0$ ppm).[12] A larger quadrupolar interaction for trigonal than for tetragonal ^{11}B sites is also expected, as observed in borates.[26] Spectra were recorded for **V** and **VI**, and examples are given in Figs 9 and 10. Simulations of the central band lineshapes yield values of isotropic chemical shifts δ_{ISO}, quadupolar coupling constants Q_{CC} and asymmetry factors η, which are summarized in Table 3: $Q_{CC} = e^2qQ/$ and $\eta = (V_{yy} - V_{xx})/V_{zz}$ where Q is the quadrupolar moment,

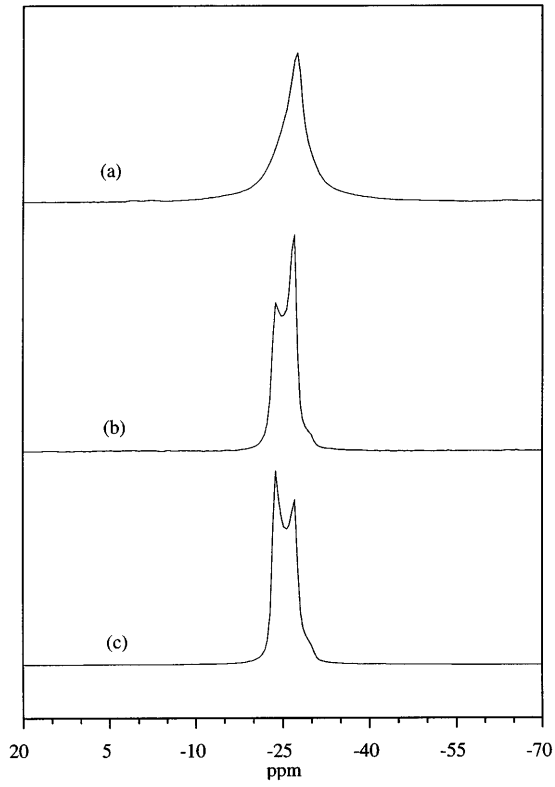

Figure 9. Experimental ^{11}B MAS spectrum of NH_3BH_3 (**Va**) recorded (a) without and (b) with proton decoupling (500 scans, $\nu_{rot} = 8$ kHz). (c) Theoretical spectrum, simulated with a second-order quadrupolar interaction ($Q_{CC} = 1.5$ MHz and $\eta = 0$).

Table 3. ^{11}B chemical shifts, quadrupolar coupling constants and asymmetry factors extracted from the ^{11}B MAS NMR spectra

Compound	δ_{iso} (^{11}B) (ppm)	Q_{CC} (MHz)	η
$NH_3 \cdot BH_3$ (**Va**)	−23	1.5	0
$MeNH_2 \cdot BH_3$ (**Vb**)	−18	1.6	0
$Me_2NH \cdot BH_3$ (**Vc**)	−15	1.4	0
$Me_3N \cdot BH_3$ (**Vd**)	−8	1.6	0
$^tBuNH_2 \cdot BH_3$ (**Ve**)	−22	1.6	0
$B_3N_3C_6H_6$ (**VI**)	24	2.8	0

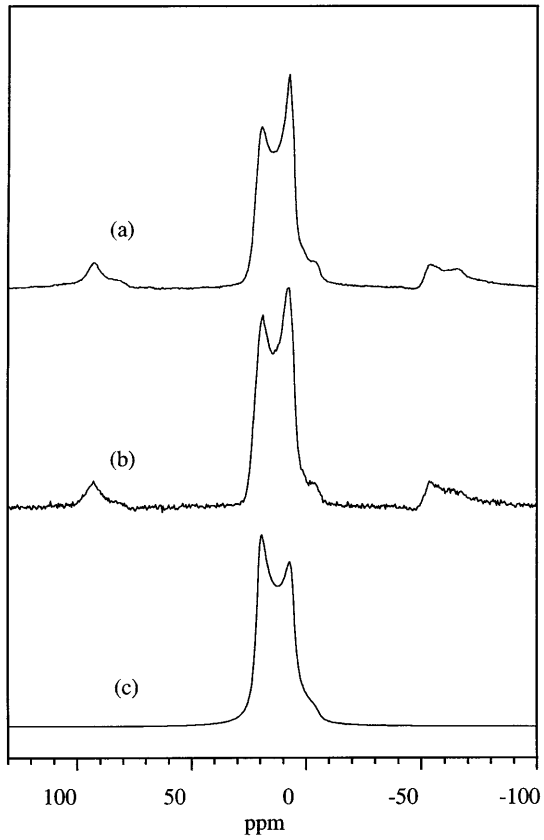

Figure 10. Experimental ^{11}B MAS spectrum of trialcynylborazine (**VI**) recorded (a) without and (b) with proton decoupling (500 scans, $\nu_{rot} = 9$ kHz). (c) Theoretical spectrum, simulated with a second-order quadrupolar interaction ($Q_{CC} = 2.8$ MHz and $\eta = 0$).

$eq = V_{zz}$ where V_{xx}, V_{yy} and V_{zz} are the principal elements of the tensor describing the electric field gradient. The isotropic chemical shifts are in good agreement with those reported in the literature[8,10] and their ranges are small but sufficient to distinguish the boron sites according to their coordination numbers: around 25–30 ppm for tricoordinated boron atoms in borazine rings and between −30 and 0 ppm for tetracoordinated boron atoms in borane–ammonia complexes. A low-field shift can also be observed through the $Me_xNH_{3-x} \cdot BH_3$ series from $x = 0$ to 3. The values of quadrupolar coupling constants are dependent on the boron site symmetry: they are smaller for the tetragonal sites ($Q_{cc} = 1.5 \pm 0.1$ MHz) than for the trigonal sites ($Q_{cc} = 2.8$ MHz), as expected. This last value is similar to that reported for h-BN ($Q_{cc} = 2.9$ MHz)[12] and is characteristic of B_3N_3 ring structures. Comparison between the isotropic chemical shifts found for **VI** and h-BN (24 *vs.* 30 ppm) shows clearly that it will be difficult, using only single quantum MAS experiments, to identify trigonal B sites with different neighboring atoms. Moreover, another feature should be pointed out concerning the shape of the center-band pattern obtained with proton decoupling.

Figure 9 shows the ^{11}B MAS NMR spectra of $NH_3 \cdot BH_3$ (**Va**). It indicates that even with rapid MAS, a well resolved spectrum is not obtained, partly owing to the remaining ^{11}B–^{1}H dipolar interaction, which can be estimated as $\omega_d/2\pi = 22.6$ kHz, with a B—H distance of 1.20 Å.[46] The ^{11}B–^{1}H dipolar interaction is removed by application of ^{1}H decoupling, and a center-band pattern, typical of a second-order quadrupolar lineshape, with a small asymmetry factor is obtained. Nevertheless, the intensities of the two maxima are inverted compared with those expected from computations taking into account second-order quadrupolar interaction alone, even with a distribution. The ^{11}B MAS NMR spectra of trialcynylborazine (**VI**) with and without proton decoupling (Fig. 10) are very similar owing to a much smaller ^{11}B–^{1}H interaction in this compound. There is still an inversion of the intensities of the maxima in the signal. The same feature was also observed in the MAS NMR spectrum of hexagonal BN recorded at 9.4 T with a spinning rate of 10 kHz.

If we consider the ^{11}B MAS NMR spectra of boric acid, $B(OH)_3$, in Fig. 11, recorded with proton decoupling, a center-band pattern without inversion of the intensities of the maxima is obtained. $B(OH)_3$ is a crystalline compound, composed of isolated $B(OH)_3$ units.[47] The only strong dipolar coupling is thus due to ^{11}B–^{1}H interactions. This may suggest that the observed inversion of intensity of the quadrupolar shape maxima in the samples containing B—N bonds might be due to the

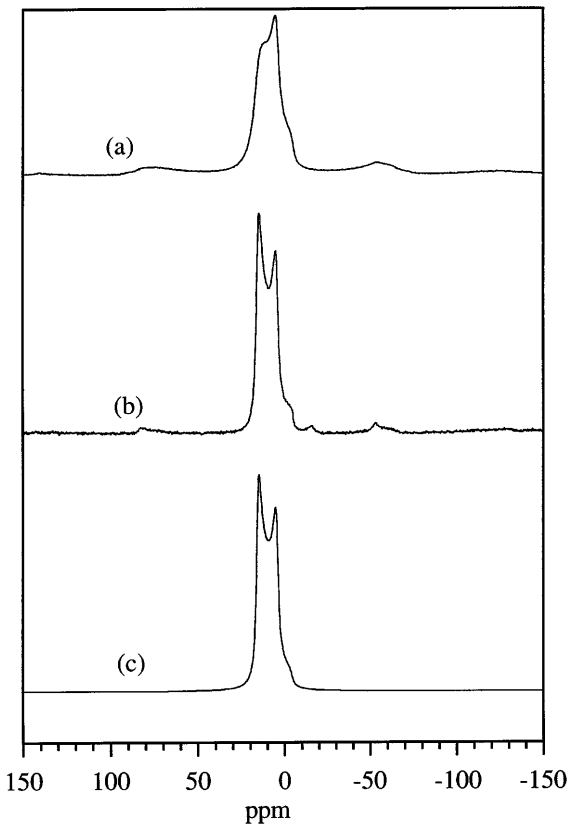

Figure 11. Experimental ^{11}B MAS spectrum of $B(OH)_3$ recorded (a) without and (b) with proton decoupling (120 scans, $\nu_{rot} = 9$ kHz). (c) Theoretical spectrum, simulated with a second-order quadrupolar interaction ($Q_{CC} = 2.5$ MHz and $\eta = 0$).

coupling of ^{11}B nuclei to neighbouring ^{14}N ($I = 1$) quadrupolar nuclei. This effect is of the same nature as those observed for spin-1/2 nuclei directly bonded to spin-3/2 or -1, with non-vanishing shapes at high MAS spinning rates.[48–51] It is predicted to be scaled down at high field.

CONCLUSION

Solid-state NMR studies of borane–ammonia complexes, trialcynylborazine and *N*-trimethylcycloborazane have been described. The primary objective was to establish whether the identification of B and N sites in compounds containing B—N bonds would be possible through ^{15}N and ^{11}B NMR experiments, in order to extend such investigation to the characterization of boron nitride pre-ceramic polymers. In such model compounds, ^{15}N and ^{11}B chemical shift values are sensitive to the coordination number of the respective N and B sites but, for a given coordination state, not so much to the nature of the neighboring atoms. The IRCP pulse sequence was applied to investigate the $^{1}H \rightarrow {}^{15}N$ polarization transfer of the $^{15}NH_x$ sites in these reference compounds and to distinguish the N sites according to their proton environment. This study demonstrates that IRCP could be a powerful tool to study boron nitride pre-ceramic polymers in order to identify the nature of the various protonated and non-protonated N sites if the observed groups are rigid. If not, the IRCP behavior will be more difficult to predict. The ^{11}B MAS NMR study shows that, besides the coordination state of the B atoms, a detailed description of the B sites is difficult in the absence of a total averaging of the quadrupolar interactions. Moreover, an unusual shape of the center band was found for all the compounds which contain at least one B—N bond. This might suggest the presence of residual second-order ^{11}B–^{14}N dipolar coupling. In the context of the study of BN preceramic polymers, the use of the MQMAS sequence will be considered in order to obtain easier access to the isotropic chemical shift values.

Acknowledgements

This work was supported by the French Ministry of Defence (DGA) (grant No. 95-2569A).

REFERENCES

1. P. J. Fazen, E. E. Remsen, J. S. Beck, P. J. Caroll, A. R. McGhie and L. G. Sneddon, *Chem. Mater.* **7**, 1942 (1995).
2. T. Wideman and L. G. Sneddon, *Inorg. Chem.* **34**, 1002 (1995).
3. J. Bill and F. Aldinger, *Adv. Mater.* **9**, 775 (1995).
4. S. Yajima, in *Handbook of Composites, Vol. 1: Strong Fibres*, edited by W. Watt and B. V. Perov. Elsevier, Amsterdam (1985).
5. R. M. Laine and F. Babonneau, *Chem. Mater.* **5**, 260 (1993).
6. M. Birot, J. P. Pillot and J. Dunogues, *Chem. Rev.* **95**, 1443 (1995).
7. G. D. Soraru, F. Babonneau and J. D. Mackenzie, *J. Mater. Sci.* **25**, 3886 (1990); W. R. Schmidt, L. V. Interrante, R. H. Doremus, T. K. Trout, P. S. Marchetti and G. E. Maciel, *Chem. Mater.* **3**, 257 (1991); C. Gérardin, F. Taulelle and D. Bahloul, *J. Mater. Chem.* **7**, 117 (1997).
8. D. F. Gaines and R. Schaeffer, *J. Am. Chem. Soc.* **86**, 1505 (1964).
9. C. W. Heitsch, *Inorg. Chem.* **4**, 1019 (1965).
10. B. Wrackmeyer, *J. Magn. Reson.* **66**, 172 (1986).
11. E. C. Reynhardt and C. F. Hoon, *J. Phys. C* **16**, 6137 (1983).
12. P. S. Marchetti, D. Kwon, W. R. Schmidt, L. V. Interrante and G. E. Maciel, *Chem. Mater.* **3**, 485 (1991).
13. A. Pines, M. G. Gibby and J. S. Waugh, *J. Chem. Phys.* **59**, 569 (1973).
14. J. Schaefer and E. O. Stejskal, *J. Am. Chem. Soc.* **98**, 1031 (1976).
15. A. E. Derome, *Modern NMR Techniques for Chemistry Research.* Pergamon Press, Oxford (1987).
16. P. Tekely, F. Montigny, D. Canet and J. J. Delpuech, *Chem. Phys. Lett.* **175**, 401 (1990).
17. X. Wu and K. W. Zilm, *J. Magn. Reson. A* **102**, 205 (1993).
18. R. Sangill, N. Rastrup-Andersen, H. Bildsoe, H. J. Jakobsen and N. C. Nielsen, *J. Magn. Res. A* **107**, 67 (1994).
19. P. Palmas, P. Tekely and D. Canet, *J. Magn. Reson. A* **104**, 26 (1993).
20. J. Hirschinger and M. Hervé, *Solid State Magn. Reson.* **3**, 121 (1994).
21. X. Wu, S. T. Burns and K. W. Zilm, *J. Magn. Reson. A* **111**, 29 (1994).
22. C. Bonhomme, F. Babonneau, J. Maquet, J. Livage, M. Vaultier and E. Framery, *J. Chim. Phys.* **92**, 1884 (1995).
23. F. Babonneau, J. Maquet, C. Bonhomme, R. Richter, G. Roewer and D. Bahloul, *Chem. Mater.* **8**, 1415 (1996).
24. C. A. Fyfe, G. C. Gobbi, J. S. Hartmann, R. E. Lenkinski, J. H. O'Brien, E. R. Beange and M. A. R. Smith, *J. Magn. Reson.* **47**, 168 (1982).
25. S. Schramm and E. J. Oldfield, *J. Chem. Soc., Chem. Commun.* 980 (1982).
26. A. H. Silver and P. J. Bray, *J. Chem. Phys.* **29**, 984 (1958).
27. P. J. Bray, *J. Non-Cryst. Solids* **95/96**, 45 (1987).
28. G. L. Turner, K. A. Smith, R. J. Kirkpatrick and E. Oldfield, *J. Magn. Reson.* **67**, 544 (1986).
29. M. Fanciulli and M. Corti, *Phys. Rev. B* **52**, 11872 (1995).
30. A. H. Silver and P. J. Bray, *J. Chem. Phys.* **32**, 288 (1960).
31. A. Llor and J. Virlet, *Chem. Phys. Lett.* **152**, 248 (1988).
32. B. F. Chmelka, K. T. Mueller, A. Pines, J. Stebins, Y. Wu and J. W. Zwanziger, *Nature* **339**, 42 (1989).
33. A. Samoson, E. Lipmaa and A. Pines, *Mol. Phys.* **67**, 1013 (1988).
34. Y. Wu, B. Q. Sun and A. Pines, *J. Magn. Reson.* **89**, 297 (1990).
35. A. Medek, J. S. Harwood and L. Frydman, *J. Am. Chem. Soc.* **117**, 12779 (1995).
36. R. E. Youngman and J. W. Zwanziger, *J. Phys. Chem.* **100**, 16720 (1996).
37. S.-J. Hwang, C. Fernandez, J. P. Amoureux, J. Cho, S. W. Martin and M. Pruski, *Solid State Magn. Reson.* **8**, 109 (1997).
38. M. G. Hu, J. M. van Paasschen and R. A. Geanangel, *J. Inorg. Nucl. Chem.* **39**, 2147 (1977).
39. C. K. Narula, J. F. Janik, E. N. Duesler, R. T. Paine and R. Schaeffer, *Inorg. Chem.* **25**, 3346 (1986).
40. C. Blanchard, E. Chassagneux, G. Mignani and M. Vaultier, *Eur. Pat.* 93 400704 8 (1993).
41. D. F. Gaines and R. Schaeffer, *J. Am. Chem. Soc.* **85**, 395 (1963).
42. D. Massiot, H. Thiele and A. Germanus, *Bruker Rep.* **140**, 43 (1994).
43. E. Framery, Thèse de l'Université de Rennes I (1996).
44. X. Wu, S. Zhang, *Chem. Phys. Lett.* **156**, 79 (1989).
45. L. B. Alemany, D. M. Grant, T. D. Alger and R. J. Pugmire, *J. Am. Chem. Soc.* **105**, 2133 (1983).
46. M. Chaillet, A. Dargelos and J. Marsden, *New. J. Chem.* **18**, 693 (1994).
47. W. H. Zachariasen, *Acta Crystallogr.* **7**, 305 (1954).
48. S. J. Opella, M. H. Frey and T. A. Cross, *J. Am. Chem. Soc.* **101**, 5856 (1979).
49. E. M. Menger and W. S. Veeman, *J. Magn. Reson.* **46**, 257 (1982).
50. D. C. Apperley, B. Haiping and R. K. Harris, *Mol. Phys.* **68**, 1277 (1989).
51. R. Challoner, R. K. Harris, *Solid State Nucl. Magn. Reson.* **4**, 65 (1995).

